

EMD Algorithm with Approximate Zero Crossings

Mayer Humi

Department of Mathematical Sciences,
Worcester Polytechnic Institute,
Worcester, MA 01609, USA *

Abstract

The classical EMD algorithm has been used extensively in the literature to decompose signals that contain nonlinear waves. However when a signal contain two or more frequencies that are close to one another the decomposition might fail. In this paper we propose a new formulation of this algorithm which is based on the zero crossings of the signal and show that it performs well even when the classical algorithm fail. We address also the filtering properties and convergence rate of the new algorithm versus the classical EMD algorithm.

Keywords: Signal Analysis, Filtering, EMD algorithm

*e-mail: mhumi@wpi.edu.

1 Introduction

In scientific literature there exist many classical sets of functions which can decompose a signal in terms of "simple" functions. For example Taylor or Fourier expansions are used routinely in scientific and engineering applications (and many other exist). However in all these expansions the underlying functions are not intrinsic to the signal itself and a precise approximation to the original signal might require a large number of terms. This problem become even more acute when the signal is non-stationary and the process it represents is nonlinear.

To overcome this problem many researchers used in the past the "principal component algorithm" (PCA) to come up with an "adaptive" set of functions which approximate a given signal. A new approach to this problem emerged in the late 1990's when a NASA team has developed the "Empirical Mode Decomposition" algorithm(EMD) which attempts to decompose a signal in terms of it "intrinsic mode functions" (IMF) through "sifting algorithm". A patent for this algorithm has been issued [1].

The EMD algorithm is based on the following quote [2]: "According to Drazin the first step of data analysis is to examine the data by eye. From this examination, one can immediately identify the different scales directly in two ways: by the time lapse between successive alterations of local maxima and minima and by the time lapse between the successive zero crossings....We have decided to to adopt the time lapse between successive extrema as the definition of the time scale for the intrinsic oscillatory mode"

A step by step description of the EMD sifting algorithm is as follows:

1. Let be given a function $f(t)$ which is sampled at discrete times $\{t_k, k = 1, \dots, n\}$.
2. let $h_0(k) = f(t_k)$.
3. Identify the max and min of $h_0(k)$.
4. Create the cubic spline curve M_x that connects the maxima points. Do the same for the minima M_n . This creates an envelope for $h_0(k)$.
5. At each time t_k evaluate the mean m_k of M_x and M_n (m_k is referred to as the sifting function).
6. Evaluate $h_1(k) = h_0(k) - m_k$.

7. If the norm of $||h_0 - h_1|| < \epsilon$ for some predetermined ϵ set the first intrinsic mode function $IMF_1 = h_1$ (and stop).
8. If the criteria of (7) are not satisfied set $h_0(k) = h_1(k)$ and return to (3) ("Sifting process").

The algorithm has been applied successfully in various physical applications [1-6]. However as has been observed by Flandrin [3] and others the EMD algorithm fails in many cases where the data contains two or more frequencies which are close to each other.

To overcome this difficulty we propose hereby a modification of the EMD algorithm by replacing steps 4 and 5 in the description above by the following:

4. find the midpoints between two consecutive maxima and minima and let N_k be the values of h_0 at these points.
5. Create the spline curve m_k that connects the points N_k .

The essence of this modification is the replacement of the mean which is evaluated by the EMD algorithm as the average of the max-min envelopes by the spline curve of the mid-points between the maxima and minima. This is in line with the observation by Drazin (which was referred to above) that the scales inherent to the data can be deduced either from the max-min or its zero crossing. In the algorithm we propose hereby we mimic the "zero-crossings" by the mid-points between the max-min.

It is our objective in this paper to justify this modification of the EMD algorithm through some theoretical work and case studies. The plan of the paper is as follows: In Sec 2 we provide theoretical justification for the new algorithm proving that it acts as a high pass filter for certain classes of signals. In Sec. 3 we provide examples of a signal composed of two or three close frequencies (with and without noise) where the classical EMD algorithm fails but the modified one yields satisfactory result. In Sec. 4 we discuss the convergence rate, resolution and related issues concerning the classical and new "midpoint algorithm". We end up with some conclusions in Sec 5.

2 Theoretical Justification

In this section we provide a theoretical justification for the proposed modified EMD algorithm by analyzing its performance on several generic signals which contain several close frequencies. However in this analysis linear, quadratic and cubic interpolating polynomials will be applied

to represent the midpoints interpolating function (instead of splines). To motivate this "replacement" we observe that the coefficients of each spline polynomial depend non-locally on the data i.e. these coefficients might change if additional data is added. On the other hand Lagrange interpolating polynomials depend only the local data.

Lemma 1: Consider a signal of the form

$$f(t) = f_1(t) + f_2(t) + f_3(t) \quad (2.1)$$

where

$$f_1(t) = \cos(\omega t), \quad f_2(t) = \cos((1 + a\epsilon)\omega t), \quad f_3(t) = \cos((1 + b\epsilon)\omega t), \quad b > a > 0, \quad 0 < \epsilon \ll 1. \quad (2.2)$$

Let the projection of the midpoint **linear interpolating function** on $f_1(t)$, $f_2(t)$, $f_3(t)$ over an interval containing five midpoints be denoted respectively by P_{11} , P_{21} , P_{31} then

$$P_{i1} = \frac{8\pi}{3} \frac{(b^2 + a^2 - ba)}{\omega} \epsilon + O(\epsilon^2)$$

and

$$P_{11} - P_{31} = \frac{248\pi}{3} \frac{(b^2 + a^2 - ba)b}{\omega} \epsilon^3 + O(\epsilon^4), \quad (2.3)$$

$$P_{11} - P_{21} = \frac{248\pi}{3} \frac{(b^2 + a^2 - ba)a}{\omega} \epsilon^3 + O(\epsilon^4), \quad (2.4)$$

$$P_{21} - P_{31} = \frac{248\pi}{3} \frac{(b^2 + a^2 - ba)(b - a)}{\omega} \epsilon^3 + O(\epsilon^4). \quad (2.5)$$

Proof: As a first step we find the approximate location of the extrema of $f(t)$ on the interval $[0, 6\pi]$. To do so we differentiate $f(t)$ and observe that due to the fact that $\epsilon \ll 1$ the locations of these points are close to $\frac{n\pi}{\omega}$. Setting $t = \frac{n\pi}{\omega} + \eta$ we expand $f'(t)$ in a Taylor series to order 2 in η around $\frac{n\pi}{\omega}$. Then we solve for η to obtain the approximate locations of the extrema points. Taking the five midpoints $\{t_1, \dots, t_5\}$ between these extrema and evaluating $f(t_i)$, $i = 1, \dots, 5$ we construct the linear interpolating function $g_1(t)$ between these points. The projection of $f_i(t)$ on $g_1(t)$ is

$$P_{i1} = \int_{t_1}^{t_5} f_i(t) g_1(t) dt. \quad (2.6)$$

Expanding $P_{i1} - P_{j1}$ in a Taylor series in ϵ one obtains (2.3)-(2.5).

Lemma 2: With the same settings as in *Lemma 1* let the function $g_2(t)$ consists of the two quadratic polynomials interpolating $\{t_1, t_2, t_3\}$ and $\{t_3, t_4, t_5\}$ respectively. The differences between the projections

$$P_{i2} = \int_{t_1}^{t_5} f_i(t)g_2(t)dt \quad (2.7)$$

are given by eqs (2.3),(2.4) and (2.5) respectively (where P_{i1} is replaced by P_{i2})

Proof: As in *Lemma 1* we compute the projections P_{i2} and expand the results in a Taylor series in ϵ to obtain (2.3)-(2.5)

Lemma 3: With the same settings as in *Lemma 1* if the projection of $f_1(t)$, $f_2(t)$, $f_3(t)$ is made on the cubic polynomial $g_3(t)$ interpolating $\{t_1, t_2, t_3, t_4\}$ then the differences between the projections

$$P_{i3} = \int_{t_1}^{t_4} f_i(t)g_3(t)dt \quad (2.8)$$

are given by

$$P_{13} - P_{33} = \frac{8}{9} \frac{b(b^2 + a^2 - ba)(49\pi^2 - 57)}{\omega\pi} \epsilon^3 + O(\epsilon^4), \quad (2.9)$$

$$P_{13} - P_{23} = \frac{8}{9} \frac{a(b^2 + a^2 - ba)(49\pi^2 - 57)}{\omega\pi} \epsilon^3 + O(\epsilon^4), \quad (2.10)$$

$$P_{23} - P_{33} = \frac{8}{9} \frac{(b-a)(b^2 + a^2 - ba)(49\pi^2 - 57)}{\omega\pi} \epsilon^3 + O(\epsilon^4). \quad (2.11)$$

Theorem 1: As a result of one iteration of the midpoint EMD algorithm with linear, quadratic or cubic interpolating functions the change in the projections of the functions $f_i(t)$ $i = 1, 2, 3$ on the signal in the interval $[t_1, t_5]$ ($[t_1, t_4]$ in the cubic case) satisfy $\Delta A_{1,j} > \Delta A_{2,j} > \Delta A_{3,j}$, $j = 1, 2, 3$. (Here j represents the different interpolating functions).

Proof: The projection of $f_i(t)$ on the original signal is

$$A_{i,j}^0 = \int_{t_1}^{t_5} f(t)f_i(t)dt.$$

After one iteration the signal is represented by

$$f^1(t) = f(t) - g_j(t)$$

and the projection of $f_i(t)$ on $f^1(t)$ is

$$A_{i,j}^1 = \int_{t_1}^{t_5} (f(t) - g_j(t))f_i(t)dt = A_{i,j}^0 - P_{i,j}.$$

Hence

$$\Delta A_{i,j} = A_{i,j}^0 - A_{i,j}^1 = P_{i,j} > 0$$

From the results of *lemmas* 1, 2, 3 we have that For $j = 1, 2, 3$ $P_{1j} - P_{2j} > 0$, $P_{1j} - P_{3j} > 0$ and $P_{2j} - P_{3j} > 0$. It follows then that $\Delta A_{1,j} > \Delta A_{2,j} > \Delta A_{3,j} > 0$.

We conclude therefore that in the new signal (after one iteration) the amplitude of $f_3(t)$ will be larger than those of $f_2(t)$ and $f_1(t)$. In other words the midpoint EMD algorithm acts as a high pass filter.

We consider now a signal with two close frequencies where a phase shifts exists between these two frequencies.

Lemma 4: Consider a signal of the form

$$f(t) = f_4(t) + f_5(t) \quad (2.12)$$

where

$$f_4(t) = \cos(\omega t), \quad f_5(t) = \cos[(1 + a\epsilon)\omega t + \phi]. \quad (2.13)$$

where $a > 0$, and $0 < \epsilon, \phi \ll 1$. With same setting as in *Lemma* 1 let the projection of the midpoint linear interpolating function (for $f(t)$ defined in (2.13)) on $f_4(t)$, $f_5(t)$ over an interval containing five midpoints $\{t_1, \dots, t_5\}$ be denoted respectively by P_{41} , P_{51} then

$$P_{41} - P_{51} = \frac{2a\epsilon[6a^2\pi^2\epsilon^2 + (5\pi a\epsilon + 2\phi)^2]}{\omega\pi} + O(\epsilon^4, \phi^4) \quad (2.14)$$

Lemma 5: With the same settings as in *Lemma* 4 let the function $g_5(t)$ consists of the two quadratic polynomials interpolating $\{t_1, t_2, t_3\}$ and $\{t_3, t_4, t_5\}$ respectively. The difference between the projections P_{42} , P_{52} of $f_4(t)$, $f_5(t)$ on $g_5(t)$ is given by (2.14) (where P_{i1} is replaced by P_{i2}).

Lemma 6: With the same settings as in *Lemma* 4 let the function $g_6(t)$ consists of the cubic polynomial interpolating $\{t_1, t_2, t_3, t_4\}$. The difference between the projections P_{43} , P_{53} of $f_4(t)$, $f_5(t)$ on $g_6(t)$ is

$$P_{43} - P_{53} = \frac{2a}{3\omega\pi^3} [a^2\pi^2(49\pi^2 - 57)\epsilon^3 + 8a\pi\phi(5\pi^2 - 6)\epsilon^2 + 2\phi^2(5\pi^2 - 6)\epsilon] + O(\epsilon^4, \phi^4) \quad (2.15)$$

Theorem 2: As a result of one iteration of the midpoint EMD algorithm with linear, quadratic or cubic interpolating functions the amplitudes $B_{i,j}$, $i = 1, 2$ $j = 1, 2, 3$ (where the index j represents the different interpolating functions) of the two frequencies present in the

signal (2.12)-2.13)) will satisfy $B_{1,j} < B_{2,j}$. In other words the midpoint EMD algorithm for this signal is a high pass filter.

Proof: The proof is similar to the proof of theorem 1.

2.1 Perturbation Analysis

To investigate the performance of the EMD algorithm (classical and midpoint) in the presence of a perturbation (viz. noise) we considered a signal of the form

$$S_0(t) = \cos(\omega t) + \epsilon f(t) \quad (2.16)$$

where $0 < \epsilon \ll 1$. To analyze this signal we assume that the presence of noise (represented by $\epsilon f(t)$) does not change (appreciably) the location of the extrema in the signal i.e. the maximum and minimum are located respectively at the following times

$$p_k = \frac{2k\pi}{\omega}, \quad q_k = \frac{(2k+1)\pi}{\omega}, \quad k = 0, 1, \dots \quad (2.17)$$

The value of the signal at these points is

$$S_0(p_k) = 1 + \epsilon f\left(\frac{2k\pi}{\omega}\right), \quad S_0(q_k) = -1 + \epsilon f\left(\frac{(2k+1)\pi}{\omega}\right), \quad k = 0, 1, \dots \quad (2.18)$$

To apply the classical EMD algorithm to this data one has to compute the spline curves $S_{max}(t)$ and $S_{min}(t)$ for the points $(p_k, S(p_k))$ and $(q_k, S(q_k))$ respectively. The new signal after one iteration of the (classical) EMD algorithm is given by

$$S_1^c(t) = S_0(t) - \frac{S_{max}(t) + S_{min}(t)}{2} \quad (2.19)$$

Similarly for the new EMD algorithm we take the midpoints $d_j = \frac{(2j+1)\pi}{2\omega}$, $j = 0, 1, \dots$ between the extrema of the signal and evaluate the signal at these points to obtain

$$S_0(d_j) = \epsilon f\left(\frac{(2j+1)\pi}{2\omega}\right). \quad (2.20)$$

Computing the spline curve S_{mid} for the data points $(d_j, S_0(d_j))$, and subtracting this from the original signal we obtain after one iteration of this algorithm that the new signal is given by

$$S_1^n(t) = S_0(t) - S_{mid}(t). \quad (2.21)$$

To compare the noise reduction efficiency of the two algorithms for this signal on a finite time interval $[0, \frac{(2n+1)\pi}{\omega}]$ (i.e $k = 0, \dots, n$ and $j = 0, \dots, 2n$) we project the new signals on $\{\cos(\omega t), \sin(\omega t)\}$. (Both $\{\cos(\omega t), \sin(\omega t)\}$ have to be considered due to a possible phase shift in the new signal). To this end we have to compute

$$P_1^c = \int_{q_0}^{p_n} S_1^c(t) \cos(\omega t) dt, \quad P_2^c = \int_{q_0}^{p_n} S_1^c(t) \sin(\omega t) dt. \quad (2.22)$$

and

$$Q_1^n = \int_{d_0}^{d_{2n}} S_1^n(t) \cos(\omega t) dt, \quad Q_2^n = \int_{d_0}^{d_{2n}} S_1^n(t) \sin(\omega t) dt. \quad (2.23)$$

Using (2.16)-(2.21) yields

$$P_1^c = \frac{\pi(k-1)}{2\omega} + \int_{q_0}^{p_n} [\epsilon f(t) - \frac{S_{max}(t) + S_{min}(t)}{2}] \cos(\omega t) dt \quad (2.24)$$

$$P_2^c = \int_{q_0}^{p_n} [\epsilon f(t) - \frac{S_{max}(t) + S_{min}(t)}{2}] \sin(\omega t) dt \quad (2.25)$$

$$Q_1^n = \frac{\pi k}{2\omega} + \int_{d_0}^{d_{2n}} [\epsilon f(t) - S_{mid}(t)] \cos(\omega t) dt \quad (2.26)$$

$$Q_2^n = \int_{d_0}^{d_{2n}} [\epsilon f(t) - S_{mid}(t)] \sin(\omega t) dt. \quad (2.27)$$

We conclude then that the efficiency of the algorithm to eliminate the noise in the signal can be measured by the smallness of the absolute values of the integrals

$$P_{mn} = \int_{q_0}^{p_n} [\epsilon f(t) - \frac{S_{max}(t) + S_{min}(t)}{2}] \cos(\omega t) dt, \quad Q_{mid} = \int_{d_0}^{d_{2n}} [\epsilon f(t) - S_{mid}(t)] \cos(\omega t) dt$$

and the absolute values of P_2^c, Q_2^n .

To obtain a quantitative insight into this issue we considered the special case where

$$f(t) = \cos(\nu t).$$

with $k = 0, \dots, 9$ and $j = 0, \dots, 18$. A calculation of the P_{mn} and the other integrals for $\nu \approx \omega$ yields:

$$\begin{aligned} P_{mn} &= \frac{26.703\epsilon}{\omega} + \frac{13.352\epsilon}{\omega^2}(\nu - \omega) + O((\nu - \omega)^2) \\ Q_{mid} &= \frac{28.274\epsilon}{\omega} + \frac{42.41\epsilon}{\omega^2}(\nu - \omega) + O((\nu - \omega)^2) \\ P_2^c &= \frac{-796.976\epsilon}{\omega^2}(\nu - \omega) + O((\nu - \omega)^2) \end{aligned}$$

$$Q_2^n = \frac{-12.207\epsilon}{\omega^2}(\nu - \omega) + O((\nu - \omega)^2)$$

These results show that when the frequency of the noise is close to the original frequency the classical algorithm leads to a large phase shift in the signal and the noise is shifted with it.

In a more general setting of this analysis one may consider a Fourier expansion of $f(t)$ if this function is periodic.

For the convergence of the sifting iteration we now prove the following:

Theorem 3: For the signal (2.16) if we replace the spline approximation between the midpoints by a linear interpolating function then the sifting process will converge to $\cos(\omega t)$ if the derivatives of $f(t)$ in the L^1 norm are bounded.

Proof: The coordinates of the the midpoints between the max-min of (2.16) are

$$d_j = (\frac{(2j+1)\pi}{2\omega}, \epsilon f(\frac{(2j+1)\pi}{2\omega})), j = 1, \dots, k+1$$

For a linear interpolation function eq. (2.21) becomes

$$S_1^n(t) = \cos(\omega t) + \epsilon \left\{ f(t) - \sum_{j=0}^k \frac{\omega \left[f(\frac{(2j+3)\pi}{2\omega}) - f(\frac{(2j+1)\pi}{2\omega}) \right] (t - \frac{(2j+1)\pi}{2\omega})}{\pi} - f(\frac{(2j+1)\pi}{2\omega}) \right\} \quad (2.28)$$

The L^1 norm of the signal $S_0(t)$ is $O(1)$. To obtain an approximation for the L^1 norm of the perturbation $P_1 = \epsilon f(t) - \omega_{mid}^1$ after one iteration we use trapezoidal integration. In this setting the integral of $f(t)$ cancels the integral of the linear interpolating function. This yields the following standard estimate for the residue of the perturbation

$$\|P_1\| = \epsilon O((\frac{\pi}{\omega})^2) \|f''(t)\|$$

(where primes denote differentiation with respect to t). We conclude that if the L^1 norm of derivatives of $f(t)$ are bounded then the sifting iterations will converge.

Using the same settings as in *theorem 3* (i.e replacing the spline interpolating function by a linear interpolating function) similar results apply to Q_1^n and Q_2^n

Lemma 7: In the L^1 norm

$$\|Q_1^n - \frac{\pi k}{2\omega}\| = \epsilon O((\frac{\pi}{\omega})^2) \|f''(t)\|, \quad \|Q_1^n\| = \epsilon O((\frac{\pi}{\omega})^2) \|f''(t)\|$$

The proof is the same as in *theorem 3*.

2.2 Some Additional Analytical Insights

To obtain analytical insights about the performance of the EMD-midpoint algorithm we considered a signal of the form

$$f(t) = \frac{1}{2}[\cos(\omega_1 t) + \cos(\omega_2 t)], \quad (2.29)$$

where the ratio of the frequencies ω_1, ω_2 is a rational number viz.

$$\frac{\omega_2}{\omega_1} = \frac{m}{n}$$

where m, n are relative prime integers. In this case the signal $f(t)$ is actually periodic with period $p = \frac{2n\pi}{\omega_1}$. Due to this fact behavior of the classical versus the mid-point algorithm can be delineated without the need to discretize the signal.

On the interval $[0, p]$ the extrema of the signal which satisfy $\frac{df}{dt} = 0$ are given by

$$\frac{\sin \omega_1 t}{\sin \omega_2 t} = -\frac{\omega_2}{\omega_1} = -\frac{m}{n}$$

Computing these extrema points it is straightforward to construct the spline approximations $S_{max}(t), S_{min}(t)$ to the maximum and minimum points and compute their average. Similarly we can find the midpoints between the maxima and minima and evaluate the corresponding spline approximation $S_{mid}(t)$ to the signal at these points. After one iteration of the sifting process the "sifted signal" is given respectively by

$$h_{mn}(t) = f(t) - \frac{S_{max}(t) + S_{min}(t)}{2}, \quad (2.30)$$

and

$$h_{mid}(t) = f(t) - S_{mid}(t). \quad (2.31)$$

The efficiency of the two algorithms can be deduced by projecting these new signals on the Fourier components of the original signal. To this end we compute

$$a_{mn} = \int_0^p h_{mn}(t) \cos(\omega_4 t) dt, \quad b_{mn} = \int_0^p h_{mn}(t) \sin(\omega_4 t) dt. \quad (2.32)$$

$$c_{mn} = \int_0^p h_{mn}(t) \cos(\omega_5 t) dt, \quad d_{mn} = \int_0^p h_{mn}(t) \sin(\omega_5 t) dt. \quad (2.33)$$

and

$$a_{mid} = \int_0^p h_{mid}(t) \cos(\omega_4 t) dt, \quad b_{mid} = \int_0^p h_{mid}(t) \sin(\omega_5 t) dt. \quad (2.34)$$

$$c_{mid} = \int_0^p h_{mid}(t) \cos(\omega_4 t) dt, \quad d_{mid} = \int_0^p h_{mid}(t) \sin(\omega_5 t) dt. \quad (2.35)$$

The amplitude of the Fourier components of the two frequencies in the classical EMD algorithm is

$$A_{mn} = \sqrt{a_{mn}^2 + b_{mn}^2}, \quad B_{mn} = \sqrt{c_{mn}^2 + d_{mn}^2}. \quad (2.36)$$

Similarly for the mid-point algorithm we

$$A_{mid} = \sqrt{a_{mid}^2 + b_{mid}^2}, \quad B_{mid} = \sqrt{c_{mid}^2 + d_{mid}^2}. \quad (2.37)$$

The objective of the sifting process is to eliminate one of the Fourier components in favor of the other. As a result the first IMF will contains, upon convergence, only one of the Fourier components in the original signal. Therefore the efficiency of the two algorithm can be inferred by comparing A_{mn} versus B_{mn} and A_{mid} versus B_{mid} .

In the particular case where the signal is given by

$$f(t) = \frac{1}{2}[\cos(\omega_1 t) + \cos(\omega_2 t)], \quad \omega_1 = \frac{3\pi}{64}, \quad \omega_2 = \frac{\pi}{32}. \quad (2.38)$$

$p = 128$ (See Fig. 5). Computing the integrals that appear in eqs. (2.32)-(2.35) we obtain

$$A_{mn} = 31.63346911, \quad B_{mn} = 29.70292046, \quad (2.39)$$

$$A_{mid} = 34.19647843, \quad B_{mid} = 20.81145369. \quad (2.40)$$

These results show that after one iteration the classical EMD did not separate the two frequencies effectively (A_{mn} and B_{mn} are close to each other). On the other hand the mid-point algorithm performed well.

3 Examples and Comparisons

Extensive numerical experiments were made to test and verify the efficiency of the modified algorithm. We present here the results of one of these tests in which the signal contains three close frequencies (where the classical EMD algorithm fails). In our tests we considered also the effects of noise and phase shifts among the different frequencies but these will not presented here.

$$f(t) = \frac{1}{3}[\cos(\omega_1 t) + \cos(\omega_2 t) + \cos(\omega_3 t)] \quad (3.1)$$

where

$$\omega_1 = 12\omega_0, \quad \omega_2 = 10\omega_0, \quad \omega_3 = 8\omega_0, \quad \omega_0 = \frac{\pi}{256}.$$

To apply the new EMD algorithm to this signal, discretized it over the time interval $[-2048, 2048]$ by letting $t_{k+1} - t_k = 1$, $k = 1, \dots, 4097$.

The results of the signal decompositions into IMFs are presented in figures 1 – 4. In all these figures the red lines represent the frequencies in the original signal (or its power spectrum) and the blue lines the corresponding intrinsic mode functions or their power spectrum which were obtained by the midpoint algorithm.

Fig. 1 is a plot of the data for the signal described by (3.1). Fig. 2 represents the first IMF in the decomposition (versus the leading frequency in the data) while Figs. 3 – 4 depict the spectral density distribution for the first two IMFs versus those related to the original frequencies in the data. It should be observed that although the amplitude of the spectral densities in these plots are somewhat different the maxima of the spectral density in each plot is very close to the original one.

3.1 Cubic Lagrange Interpolation

In both classical and the new versions of the EMD algorithm splines are used for interpolation purposes. However the coefficients of each spline polynomial depend non-locally on the data. As a result these coefficients might change if additional data is added. To compare the two algorithm without this non-local dependence we replaced the spline interpolation by cubic Lagrange interpolation (where the coefficients of the interpolating polynomial depend on the local values of the function on the interval).

To carry out this comparison between the two EMD algorithms we considered a signal composed of two frequencies and noise,

$$S_0(t) = \cos(\omega t) + \cos\left(\frac{3}{2}\omega t\right) + \epsilon f(t), \quad \epsilon \ll 1, \quad (3.2)$$

on the time interval $[0, \frac{5\pi}{\omega}]$. The time interval was chosen so that the signal (without the perturbation) has four maxima and minima on this interval.

As in subsection 2.1, we assume that the locations of the maxima and minima do not change appreciably due to the perturbation. These locations are then given respectively by

$$p_0 = 0, \quad p_1 = \frac{2}{\omega} \left(\pi - \arctan \left(\frac{\sqrt{25 - 2\sqrt{10}}}{1 + \sqrt{10}} \right) \right), \quad p_2 = \frac{4\pi}{\omega} - p_1, \quad p_3 = \frac{4\pi}{\omega}, \quad (3.3)$$

$$q_0 = \frac{2}{\omega} \left(\arctan \left(\frac{\sqrt{25 + 2\sqrt{10}}}{-1 + \sqrt{10}} \right) \right), \quad q_1 = \frac{4\pi}{\omega}, \quad q_2 = \frac{4\pi}{\omega} - q_0, \quad q_3 = \frac{4\pi}{\omega} + q_0. \quad (3.4)$$

Computing the cubic Lagrange interpolating polynomials L_{max} and L_{min} for the maxima and minima respectively we obtain for the "modified Lagrange classical-EMD" after one iteration

$$S_1^c(t) = S_0(t) - \frac{L_{max}(t) + L_{min}(t)}{2}. \quad (3.5)$$

The number of midpoints on the interval $[0, \frac{5\pi}{\omega}]$ is seven. For this reason we use two cubic Lagrange interpolating polynomials on this interval. (The first is valid over the interval $[d_0, d_3]$ and the second is valid over $[d_3, d_6]$). Denoting this combined polynomial by L_{mid} and subtracting from the original signal we obtain after one iteration of this algorithm that the new signal is given by

$$S_1^n(t) = S_0(t) - L_{mid}(t). \quad (3.6)$$

To examine the performance of the two algorithms we project these new signals on $\cos(\frac{3}{2}\omega t)$ and $\sin(\frac{3}{2}\omega t)$.

$$P_1^c = \int_{q_0}^{p_3} S_1^c(t) \cos(\frac{3}{2}\omega t) dt, \quad P_2^c = \int_{q_0}^{p_3} S_1^c(t) \sin(\frac{3}{2}\omega t) dt. \quad (3.7)$$

and

$$Q_1^n = \int_{d_0}^{d_6} S_1^n(t) \cos(\frac{3}{2}\omega t) dt, \quad Q_2^n = \int_{d_0}^{d_6} S_1^n(t) \sin(\frac{3}{2}\omega t) dt. \quad (3.8)$$

Furthermore if we assume that $f = \cos(\nu t)$ and $\nu \approx \frac{3}{2}\omega$ we obtain to order ϵ

$$P_1^c = \frac{3.8568}{\omega} + \frac{0.0175\epsilon}{\omega} + O(\nu - \frac{3}{2}\omega), \quad P_2^c = -\frac{1.0637}{\omega} + \frac{0.0399\epsilon}{\omega} + O(\nu - \frac{3}{2}\omega) \quad (3.9)$$

$$Q_1^n = \frac{6.3795}{\omega} - \frac{0.1257\epsilon}{\omega} + O(\nu - \frac{3}{2}\omega), \quad Q_2^n = -\frac{0.2184}{\omega} + \frac{0.3113\epsilon}{\omega} + O(\nu - \frac{3}{2}\omega). \quad (3.10)$$

These results demonstrate the superiority on the midpoint algorithm in this setting. (The total projection of the new signal on $\cos \frac{3}{2}\omega t$ is larger and the phase shift is smaller).

4 Convergence Rates

To compare the convergence rates of the classical versus the midpoint algorithm we considered three cases all of which were composed of two frequencies. In the first case the two

frequencies were well separated. In the second case the two frequencies were close while in the third case they were almost "overlapping". In all cases the signal was given by

$$f(t) = \frac{1}{2}(\cos \omega_1 t + \cos \omega_2 t)$$

This signal was discretized on the time interval $[-2048, 2048]$ with $\Delta t = 1$.

For the first case the two frequencies were

$$\omega_1 = 12\omega, \quad \omega_2 = 8\omega, \quad \omega = \frac{\pi}{256}.$$

As can be expected both the classical and midpoint algorithm were able to discern the individual frequencies through the sifting algorithm. However it took the classical algorithm 59 iterations to converge to the first IMF. On the other hand the midpoint algorithm converged in only 7 iterations (using the same convergence criteria). We wish to point out also that the midpoint algorithm has a lower computational cost than the classical algorithm. It requires in each iteration the computation of only one spline interpolating polynomial. On the other hand the classical algorithm requires two such polynomials, one for the maximum points and one for the minimum points.

For the second test the frequencies were

$$\omega_1 = \frac{\pi}{24} + \frac{\pi}{288}, \quad \omega_2 = \frac{\pi}{24} - \frac{\pi}{288}$$

that is the difference between the two frequencies is $\frac{\pi}{144}$.

In this case the midpoint algorithm was able to separate the two frequencies. Fig 6 and Fig 7 compare the power spectrum of the original frequencies versus those of IMF_1 and IMF_2 which were obtained through this algorithm. Convergence to IMF_1 was obtained in 18 iterations and IMF_2 was obtained by 7 additional iterations.

The classical EMD algorithm did converge to IMF_1 in 45 iterations but the power spectrum of this IMF deviated significantly from the first frequency in the signal. IMF_2 failed (completely) to detect correctly the second frequency.

In third case the frequencies were

$$\omega_1 = \frac{\pi}{24} + \frac{\pi}{1000}, \quad \omega_2 = \frac{\pi}{24} - \frac{\pi}{1000}.$$

In this case the classical algorithm was unable to separate the two frequencies i.e IMF_1 contained both frequencies. The midpoint algorithm did somewhat better but the resolution

was not complete. Moreover the sifting process in both cases led to the creation of "ghost frequencies" which were not present in the original signal.

At this juncture one might wonder if a "hybrid algorithm" whereby the sifting function is the average (or some similar combination) of those obtained by the classical and midpoint algorithms might outperform the separate algorithms (in spite of the obvious additional computational cost). However our experimentations with such algorithm did not yield the desired results (i.e. the convergence rate and resolution did not improve).

5 Conclusion

In this paper we presented a variant of the EMD algorithm which utilizes the midpoints between the max-min points of the signal in the sifting iterative process. We demonstrated through several case studies and theoretical approximations that this algorithm can resolve signals with moderately close frequencies where the classical EMD algorithm fails. We showed also that it has a better convergence rate. From a formal point of view this superior performance of the midpoint algorithm can be traced to the fact that the deviation of the signal average from zero is sampled at "half" the scale of the classical EMD algorithm.

References

- 1 N. E. Huang - USA Patent #6,311,130B1 , Date Oct 30,2001
- 2 N. E. Huang et all, "The empirical mode decomposition and the Hilbert spectrum for nonlinear and non-stationary time series analysis", Proceedings of the Royal Society Vol. 454 pp. 903-995 (1998)
- 3 Gabriel Rilling and Patrick Flandrin, "One or Two Frequencies? The Empirical Mode Decomposition Answers", IEEE Trans. Signal Analysis Vol. 56 pp.85-95 (2008).
- 4 Zhaohua Wu and Norden E. Huang, "On the Filtering Properties of the Empirical Mode Decomposition, Advances in Adaptive Data Analysis", Volume: 2, Issue: 4 pp. 397-414. (2010)

- 5 Albert Ayenu-Prah and Nii Attoh-Okine, “A Criterion for Selecting Relevant Intrinsic Mode Functions in Empirical Mode Decomposition”, *Advances in Adaptive Data Analysis*, Vol. 2, Issue: 1(2010) pp. 1-24.
- 6 G. Rilling, P. Flandrin and P. Goncalves, “Empirical Mode Decomposition As a Filter Bank, *IEEE Signal Processing Letters*, vol. 11, no. 2, pp. 112-114, 2004

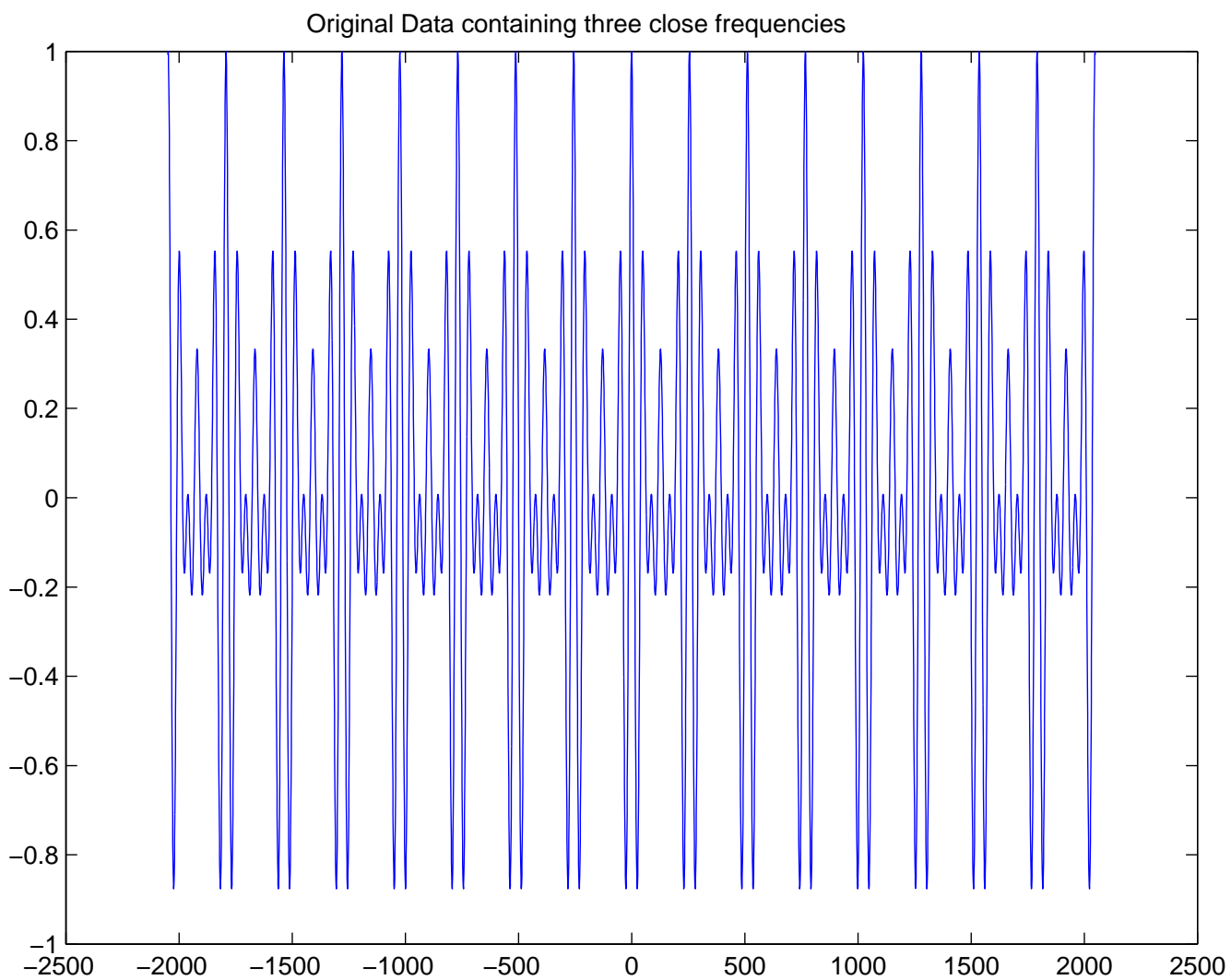


Figure 1:

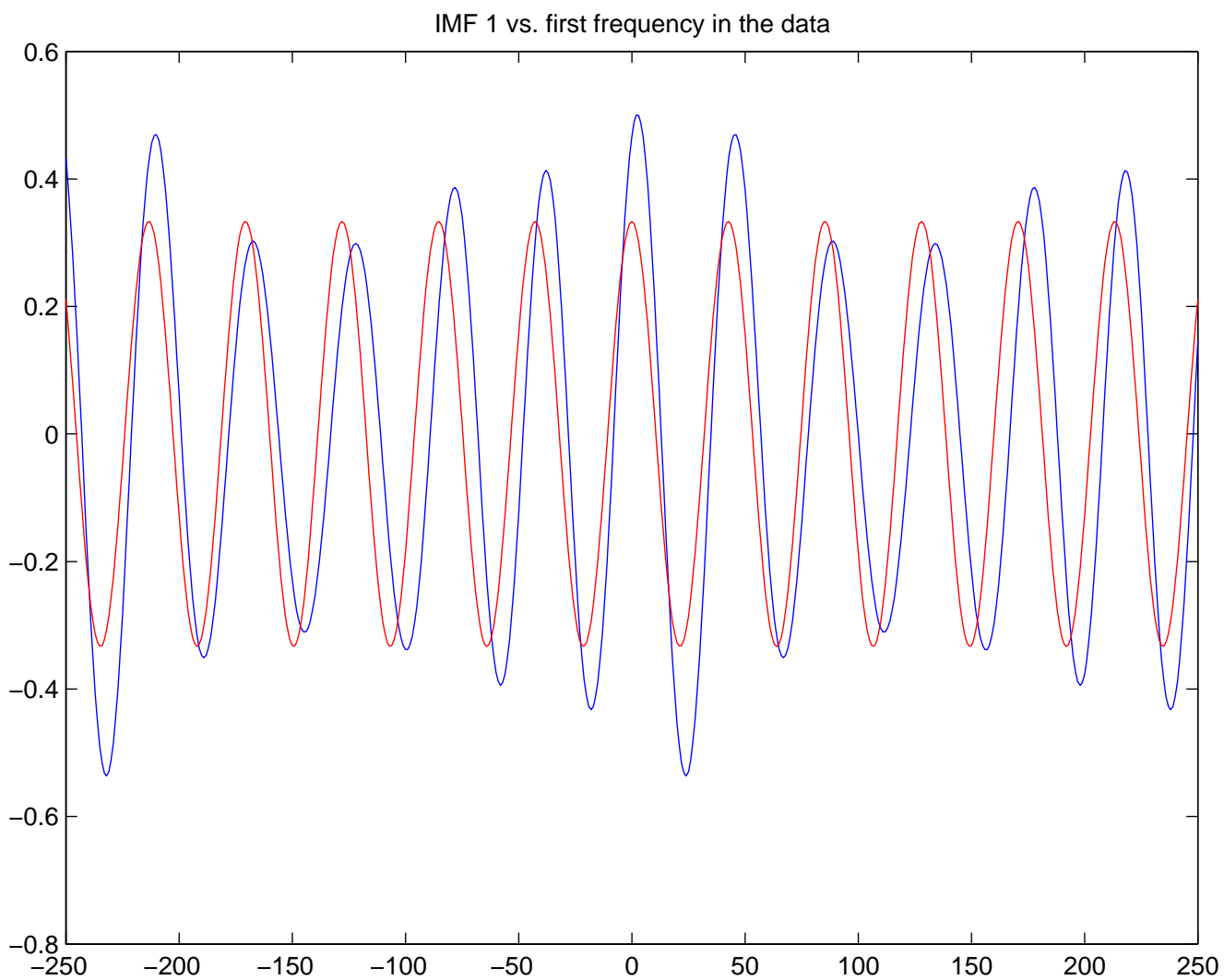


Figure 2:

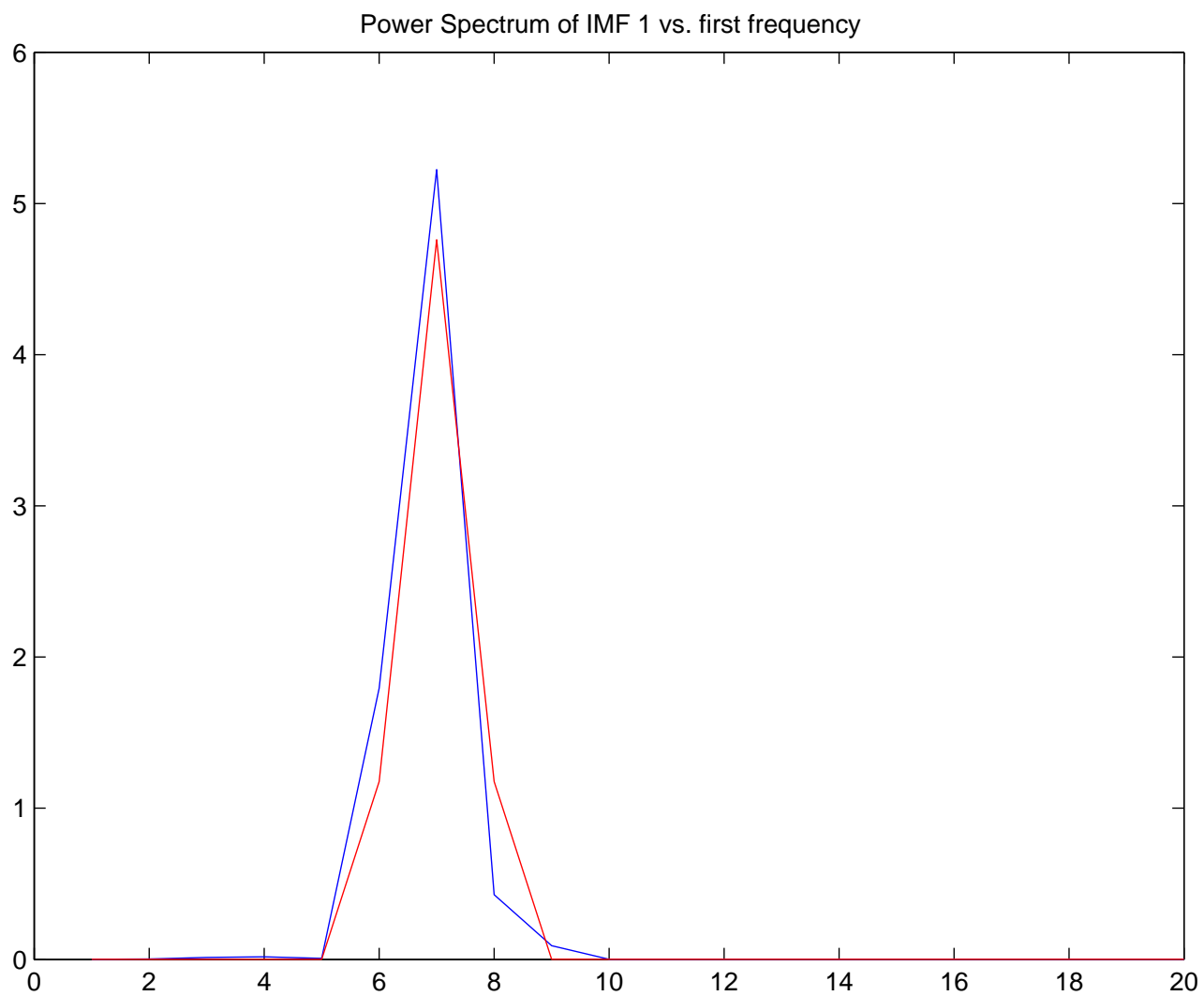


Figure 3:

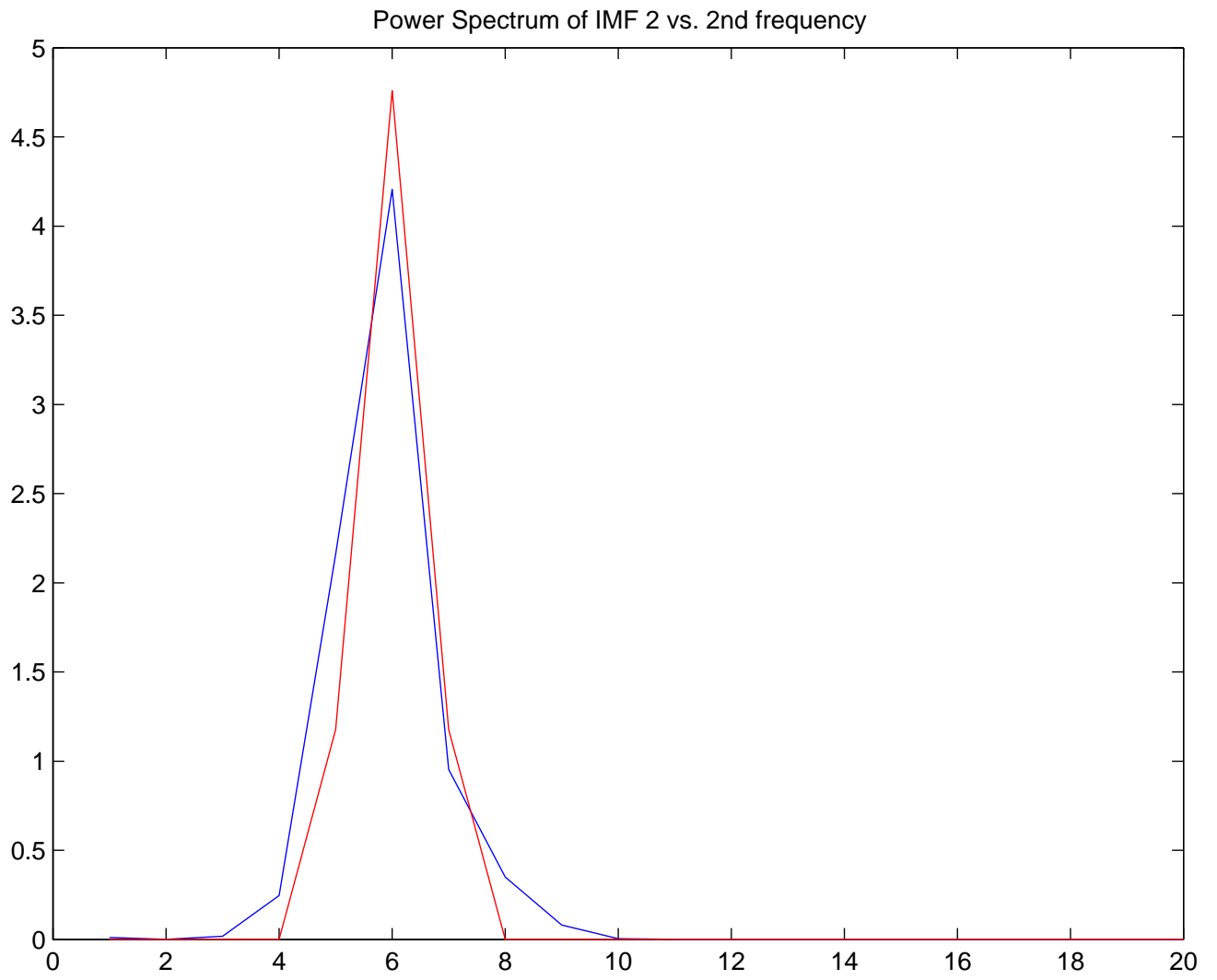


Figure 4:

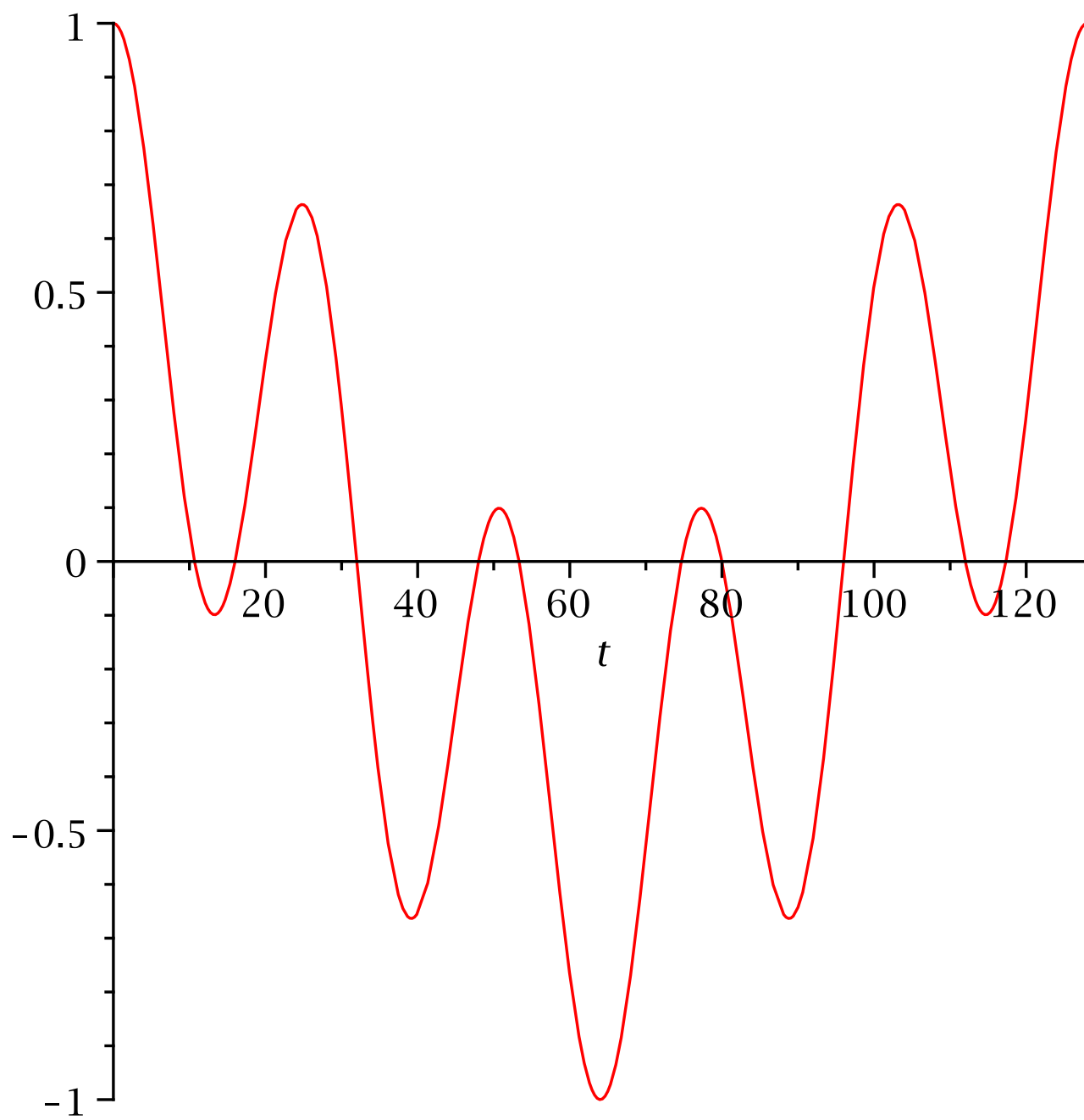


Figure 5:

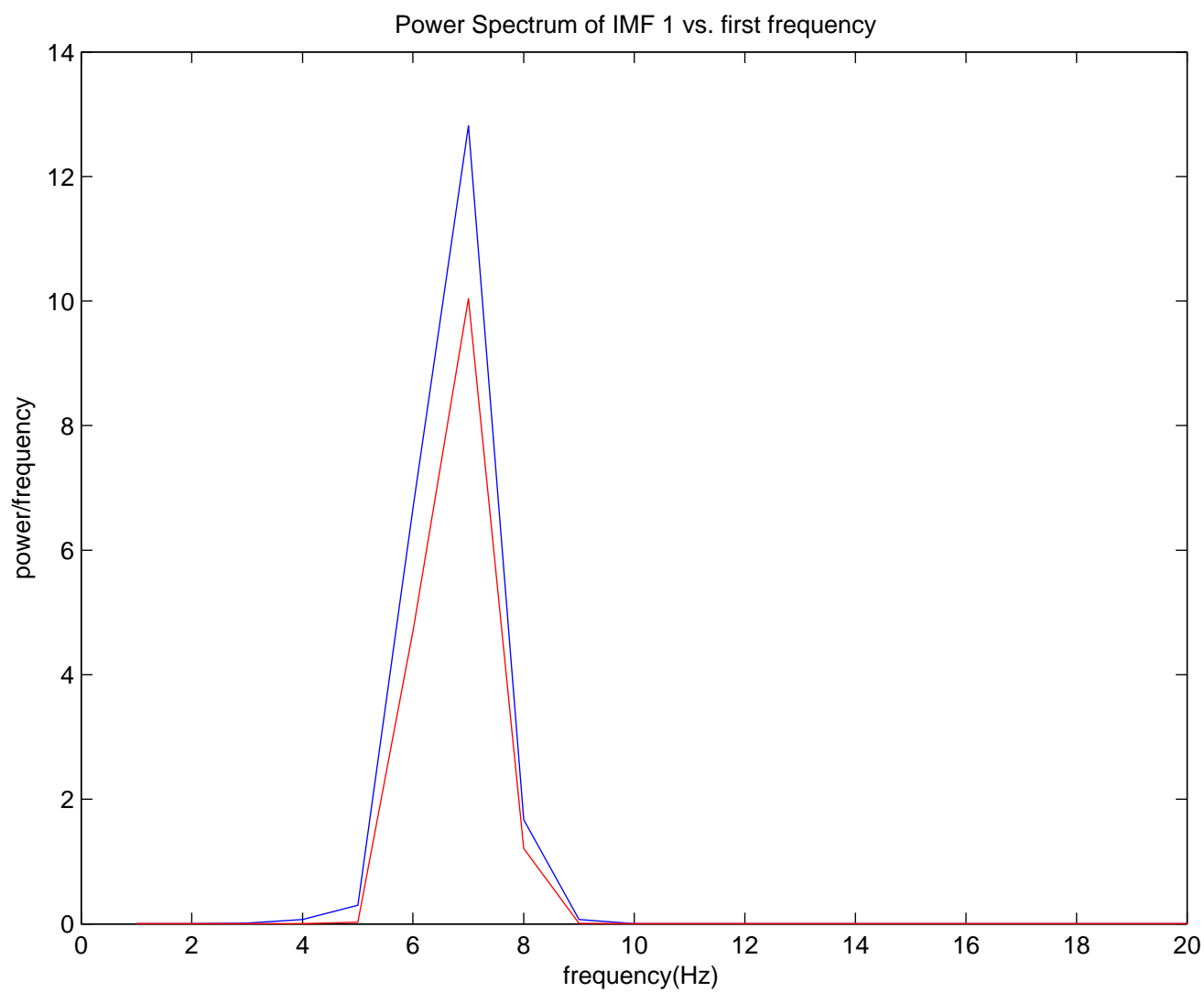


Figure 6:

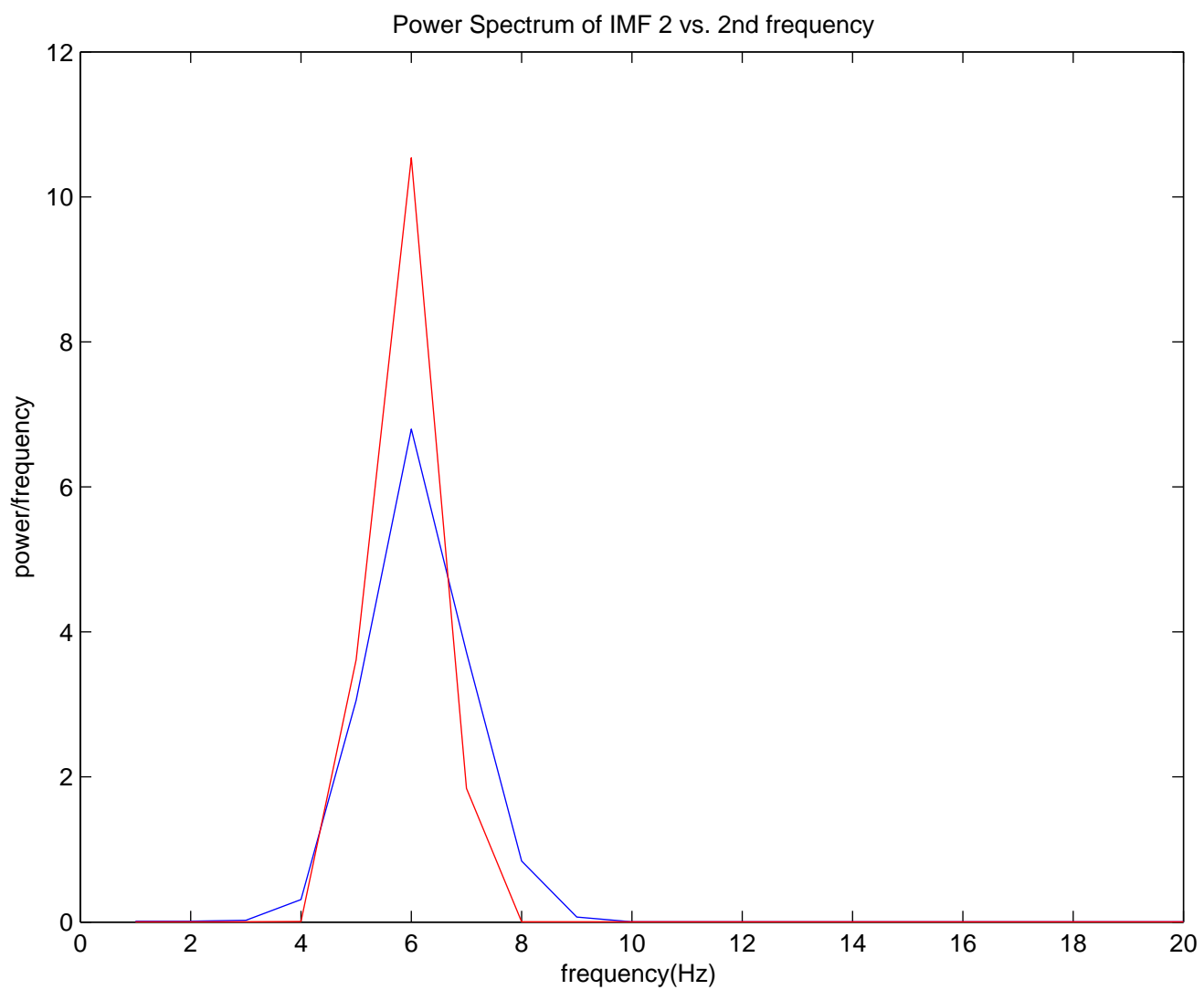


Figure 7: